HHS Public Access

Author manuscript

Nat Methods. Author manuscript; available in PMC 2016 May 18.

Published in final edited form as:

Nat Methods. 2015 December ; 12(12): 1191–1196. doi:10.1038/nmeth.3626.

Continuously Tunable Nucleic Acid Hybridization Probes

Lucia R. Wu[1,*], **J. Sherry Wang**[1,2,*], **John Z. Fang**[1], **Emily Reiser**[1], **Alessandro Pinto**[1], **Irena Pekker**[3], **Richard Boykin**[3], **Celine Ngouenet**[3], **Philippa J. Webster**[3], **Joseph Beechem**[3], and **David Yu Zhang**[1,2]

[1]Department of Bioengineering, Rice University, Houston, TX

[2]Systems, Synthetic, and Physical Biology, Rice University, Houston, TX

[3]Nanostring Technologies, Seattle, WA

Abstract

In silico designed nucleic acid probes and primers often fail to achieve favorable specificity and sensitivity tradeoffs on the first try, and iterative empirical sequence-based optimization is needed, particularly in multiplexed assays. Here, we present a novel, on-the-fly method of tuning probe affinity and selectivity via the stoichiometry of auxiliary species, allowing independent and decoupled adjustment of hybridization yield for different probes in multiplexed assays. Using this method, we achieve near-continuous tuning of probe effective free energy (0.03 kcal·mol^{-1} granularity). As applications, we enforced uniform capture efficiency of 31 DNA molecules (GC content 0% – 100%), maximized signal difference for 11 pairs of single nucleotide variants, and performed tunable hybrid-capture of mRNA from total RNA. Using the Nanostring nCounter platform, we applied stoichiometric tuning to simultaneously adjust yields for a 24-plex assay, and we show multiplexed quantitation of RNA sequences and variants from formalin-fixed, paraffin-embedded samples (FFPE).

Oligonucleotide probes and primers are used for detecting and quantitating nucleic acids, in genomics discovery and in molecular diagnostics[1,2,3]. Methods in molecular biology and analytic biochemistry have evolved, but the use of probes has only increased. In particular, with the advent of high throughput techniques[4,5,6], there is an even greater demand for probes that function reliably in a highly multiplexed setting.

Corresponding Author: David Yu Zhang, ; Email: dyz1@rice.edu

*Equal contribution authors

Author contributions. LRW, JSW, and DYZ conceived the project. LRW, JSW, and DYZ performed theoretical analysis on stoichiometric tuning. LRW, JSW, ER, JZF, AP, IP, RB, PJW, and DYZ designed and conducted experiments. LRW, JSW, JZF, AP, IP, RB, PJW, JB, and DYZ analyzed the data. LRW, JSW, and DYZ wrote the paper with input from all authors. LRW and JSW contributed equally to this work.

Conflicts of Interest. There are two patents pending on this work (PCT/US14/52827 and US provisional 62/148,555). JSW and DYZ are significant equity holders of Searna Technologies. IP, RB, CN, PJW, and JB are employees of Nanostring Technologies.

Additional information. Supplementary Notes 1–13 show additional supporting theoretical analysis and experimental data. Supplementary Note 14 shows Matlab source code for probe design and stoichiometry guidance. Supplementary Note 15 shows all oligonucleotide sequences used in experiments performed in this paper. Sequence design software is available online at http://nablab.rice.edu/nabtools/. The user's manual for the online software is available both online and as attached PDF documentation.

Probe design considers binding affinity (sensitivity) and sequence selectivity (specificity) as opposing goals; improvement in one axis generally leads to deterioration in the other[7,8,9]. Molecular assays typically seek a compromise solution with acceptable levels of both specificity and sensitivity. However, reliable *in silico* design of probes that achieve this tradeoff has heretofore eluded researchers[10,11], particularly in highly multiplexed settings[12,13], due to imperfect DNA biophysical models and parameters[14,15,16] and the intractability of analyzing complex mixtures. Empirical adjustment of operational conditions and probe sequences are typically used to optimize assay performance, but such methods can be expensive and time-consuming in multiplexed settings.

Here, we present a new method to control nucleic acid probe specificity and sensitivity, based on the stoichiometry of an auxiliary oligonucleotide. Unlike traditional probe optimization based on iterative redesign and resynthesis, our method allows on-the-fly adjustment of binding yield and selectivity with the same molecules. Furthermore, because stoichiometry can be controlled to within 5% (pipetting error), our stoichiometric tuning method allows fine control over effective reaction free energy (0.03 kcal·mol^{-1} granularity). Finally, compared to assay temperature and salinity adjustment, stoichiometric tuning allows independent modulation of probe yields in multiplexed settings. We show proof-of-concept experiments in several applications: uniform yield capture of 31 DNA targets, differential signal maximization for 11 pairs of single nucleotide variants, tunable hybrid-capture of mRNA from total RNA, and multiplexed detection of RNA variants.

Tuning Theory

The hybridization of a nucleic acid target T to a probe C can be written as $T + C <=> TC$, and has a reaction standard free energy ΔG^o_{rxn}. Probes with more negative ΔG^o_{rxn} bind with higher affinity or yield, but also spuriously binds other nucleic acid sequences [9]. Conversely, probes with less negative ΔG^o_{rxn} bind their targets with low yield but high selectivity. Probes with intermediate values of ΔG^o_{rxn} exhibit simultaneously reasonable yield and selectivity[15,16,17,18].

One major challenge in probe design is the inaccuracy and incompleteness of the literature-reported nucleic acid thermodynamics parameters and models. For a typical 25 nucleotide (nt) probe, the real ΔG^o_{rxn} value may differ from the predicted value by up to 2.4 kcal·mol^{-1} (95% confidence interval)[15], and the melting temperature Tm similarly may differ from the predicted value by up to 4 °C[10,15]. Sequence tuning is the iterative adjustment of probe length or sequence to achieve more positive or negative ΔG^o_{rxn} (Supplementary Note 1)[9]. The "granularity" of such sequence tuning is determined by the ΔG^o_{rxn} change due to a single base extension or deletion. At 25 °C in 0.15 M Na^+ (1× PBS), the granularity ranges between 0.64 and 2.32 kcal·mol^{-1}, depending on the identities of the bases at the two ends of the probe (Fig. 1a).

Here, we present stoichiometric tuning, an on-the-fly method of tuning probe yield and selectivity based on the relative concentration of an auxiliary species. Stoichiometric tuning is possible for any "double block" probe PC, such as the toehold probe[7] or the X-probe[8], that releases an auxiliary protector molecule P upon hybridization to its target T (Fig. 1b).

The equilibrium yield of the hybridization reaction ($T + PC <=> TC + P$) is defined as $\chi \equiv ([TC]_{eq} / \min\{[T]_0, [PC]_0\})$, where $[TC]_{eq}$ represents the equilibrium concentration of TC, and $[T]_0$ and $[PC]_0$ represent the initial concentrations of T and PC, respectively.

For ease of considering reaction behavior, we introduce effective reaction free energy ΔG_{eff}, a non–linear mapping of reaction yield χ: $\Delta G_{eff} \equiv -R\tau \ln(\chi / (1 - \chi))$. R is the universal gas constant and τ is the temperature in Kelvin. $\Delta G_{eff} > 0$ means that the reaction is not favorable and $\chi < 50\%$. Intuitively, the value of ΔG_{eff} usually tracks that of ΔG^o_{rxn}; a constant numerical change in ΔG^o_{rxn} usually results in a quantitatively similar change in ΔG_{eff} (Supplementary Note 2).

We calculated the analytic solution values of χ and ΔG_{eff} for a toehold probe with $\Delta G^o_{rxn} = -2$ kcal·mol^{-1} (Fig. 1c and Supplementary Note 3). Regardless of the relative concentrations of target and probe (Y-axis), excess protector stoichiometry $[P]_0/[PC]_0$ can be modulated to allow hybridization yields between essentially 0% and 100%. As an important case, when there is an excess of probe over target ($[T]_0/[PC]_0 < 1$) and when there is at least 1× excess of protector ($[P]_0/[PC]_0 > 1$), hybridization yield is dependent only on protector stoichiometry $[P]_0/[PC]_0$, and is unaffected by target or probe concentration. Consequently, samples with unknown target concentrations can be easily and quantitatively analyzed.

Stoichiometry $[P]_0/[PC]_0$ can be adjusted during probe formulation, and furthermore can be modified in real-time by addition of extra P. This results in a continuous achievable ΔG_{eff} range of roughly 10 kcal·mol^{-1} corresponding to yields between 0.02% and 99.98% ($\Delta G_{eff} = \pm 5$ kcal·mol^{-1}, respectively), with roughly 0.03 kcal·mol^{-1} granularity (5% total pipetting error).

Experimental results

Probe Sequence Design

We designed the sequences of the probes and protectors based on the thermodynamic parameters in ref. [15] and design principles in ref. [7]. To facilitate readers to design and stoichiometrically tune their own probes, we have developed a software package for automating probe design, based on a user-inputted target sequence, available online at http://nablab.rice.edu/nabtools. This software package also provides guidance on protector stoichiometry predicted to be needed for achieving a desired yield. See also Supplementary Software Manual.

Stoichiometric Tuning Validation

We designed our first toehold probe to bind its target (a subsequence of the *S. aureus mecA* gene) with $\Delta G^o_{rxn} = -2.05$ kcal·mol^{-1} (25 °C, 1× PBS); $\Delta G_{eff} = 0$ is predicted to occur when $[P]_0/[PC]_0 = 46.3$. The probe is functionalized with a TAMRA fluorophore on the C strand, and an Iowa Black RQ quencher on the P strand. When the target hybridizes to the initially dark probe, the quencher-labeled protector is displaced, and the solution fluorescence increases.

Holding $[PC]_0$ and $[T]_0$ constant, we adjusted the concentration of free protector $[P]_0$ to modulate ΔG_{eff} and yield (Fig. 1d). Experimental results were quantitatively consistent with our analytical predictions; inferred experimental yields varied between 12.2% ($[P]_0/[PC]_0$ = 1,000) and 97.4% ($[P]_0/[PC]_0$ = 1). Every factor of 3 change in $[P]_0/[PC]_0$ alters ΔG_{eff} by roughly 0.65 kcal·mol^{-1}, and 4.7% changes in $[P]_0/[PC]_0$ (ΔG_{eff} changes of 0.027 kcal·mol^{-1}) resulted in 2% yield changes. Standard deviations observed were somewhat high, due to factors such as cuvette variability, nonspecific DNA adsorption, pipetting error, and plasticware liquid retention. However, the relative ordering of mean fluorescence intensities for the 6 stoichiometries were as expected, corresponding to a p-value of 1/720 = 0.0014.

For comparison, we also show experimental results for sequence tuning of the toehold probe, via the resynthesis of a new protector molecule (red cross). A single nucleotide (G) extension of the protector resulted in a decrease of yield from 60.8% to 9.6%, corresponding to a ΔG_{eff} change of 1.59 kcal·mol^{-1}, due to a similar magnitude change in ΔG^{o}_{rxn} (Fig. 1d).

Yield can usually be calculated through a paired control experiment with unprotected probes. In assays where yield cannot be accurately measured, stoichiometric tuning can be effectively applied after collecting raw signal at two different $[P]_0/[PC]_0$ ratios. The second $[P]_0/[PC]_0$ data point allows us to fit the scaling constant mapping signal to yield (Supplementary Note 4).

Uniform capture efficiency

For enrichment applications, uniform capture yields for many different target sequences would facilitate relative and absolute quantitation. Commercial enrichment kits often show considerable biases in capture yield, particularly for sequences with very high or low GC content[19]. We designed 31 different target sequences and probes with GC content varying uniformly between 0% and 100%. Here, we used the X-probe architecture to facilitate economical testing[8]; X-probes utilize universal fluorophores and quencher oligonucleotides, but are otherwise similar to toehold probes and can likewise be stoichiometrically tuned (Supplementary Note 5).

Initially, we observed yields varying between 3% and 50% (Fig. 2abc), even though all probes were designed for 30% yield. We performed one round of sequence tuning based on observed yields to attempt to build a new probe set with uniform 30% yield, but experimental yields varied between 13.3% and 61.3%. Through the course of two rounds of stoichiometric tuning (Supplementary Note 5), we were able to dramatically tighten the yield distribution to the range of 26.6% to 36.8%, reducing the high-to-low yield variability by nearly 10-fold (Fig. 2a). Notably, predictable and uniform capture yield was achieved even for target sequences at the extremes of GC content, and uniformity was preserved in the presence of 100 ng of genomic DNA (NA18562, Coriell) corresponding to a more than 6× excess over target. Nonspecific capture of sequences similar to the target was minimal (Fig. 2d).

SNV Discrimination

Single nucleotide variations (SNVs) are clinically important because of their contributions to disease susceptibility[20]. SNV probes exemplify the challenge of balancing yield and selectivity because of the small thermodynamic change ($\Delta\Delta G^o$) associated with a single nucleotide mismatch (Fig. 3a). Based on a simple reaction analysis (Supplementary Note 6), optimal yield difference ($\Delta\chi$) is achieved when ΔG_{eff} of the correct target satisfies $\Delta G_{eff} \approx -\Delta\Delta G^o/2$ (Fig. 3b). Because $\Delta\Delta G^o$ values vary between +1 and +6 kcal·mol^{-1} based on sequence, different SNV pairs require different ΔG_{eff} values for optimal discrimination.

We measured the difference in fluorescence signals produced by a toehold probe when reacted with its DNA target versus 11 SNVs (Fig. 3c). Based on these results, we calculated the ΔG^o_{rxn} of the toehold probe with the intended target and with each SNV, from which we numerically calculated the $\Delta\Delta G^o$ of each SNV pair. From this, we calculated the $[P]_0/[PC]_0$ stoichiometry needed for achieving $\Delta G_{eff} = -\Delta\Delta G^o/2$ for each individual SNV. Following tuning, the yield difference was improved from 17.2 – 83.3% to 47.0 – 88.6% (Fig. 3d). Similar results were obtained for RNA SNV pairs (Supplementary Note 6). Note that the toehold probe used here was already near optimal; a probe less fortunately designed would have exhibited larger improvement in yield difference.

Stoichiometric tuning allows high SNV discrimination at a uniform set of temperature and buffer conditions that is difficult to achieve with other molecular probes. We compared the performance of X-probes and molecular beacons[21] in the detection of 4 cancer driver mutation sequences (Fig. 3e–f and Supplementary Note 7). There is not a single temperature in which all 4 molecular beacons yield both high sensitivity (high signal for SNV target) and high specificity (low signal for WT). Stoichiometrically tuned X-probes, despite design error in ΔG^o_{rxn}, achieves uniform ≈50% yield for all 4 probes across all 3 temperatures tested.

Multiplexed and decoupled tuning

To show decoupled tuning of 2 different probes, we constructed probes labeled with spectrally distinct fluorophores (Alexa 488 and Alexa 647). Initial stoichiometry $[P]_0/[PC]_0 = 50$ resulted in yields of 5% and 64% (Fig. 4a). Adjusting $[P]_0/[PC]_0$ to 0.765 and 208 allowed the yields of both probes to reach ≈40%. Addition of formamide, in contrast, reduces both yields.

Next, we performed multiplexed hybrid-capture of two mRNA transcripts, *ACTB* and *EIF4A2*, from human total RNA (Fig. 4b). The capture yields of the probes are assayed through reverse transcriptase quantitative PCR. Increased $[P]_0/[PC]_0$ decreased capture yield, as expected. Yields could be tuned over a range of 7.2% to 96.9%, based on quantitation cycle threshold *Cq* (Fig. 4c and Supplementary Note 8).

Multiplexed RNA analysis

We used the Nanostring nCounter platform and the Elements™ assay[22] to demonstrate highly multiplexed quantitation and tuning (Fig. 5a and Supplementary Note 9). First, all 192 probeA's in the standard Nanostring Elements gene expression panel were modified to include new nonhomologous regions to accommodate protectors. Protectors were designed

to produce 50% yield at $[P]_0/[PC]_0 = 2$. Observed yields on experiments with RNA extracted from formalin-fixed, paraffin-embedded (FFPE) tissue samples were calculated as $\text{Counts}_{\text{Toehold}}/\text{Counts}_{\text{Unprotected}}$ (Fig. 5b). For roughly 25% of the probes, the toehold probes actually produced higher counts than the unprotected ProbeA, resulting in calculated >100% yield. We interpret this to mean that the hybridization of the unprotected ProbeA to its RNA target has not reached completion, and that toehold probes hybridize to targets more rapidly than single-stranded probes.

We performed multiplexed sequence tuning for a 60-plex panel for fusion transcripts commonly associated with leukemia (Fig. 5c). Protectors with ΔG^{o}_{rxn} values 1, 2, and 3 kcal·mol^{-1} more favorable than the reference protectors were designed. Although most probes behaved as expected, with more truncated probes yielding higher signals, a small fraction resulted in unpredictable or ineffective yield tuning. These results are unlikely to be due to nonspecific target-probe binding; target to probe signals appeared orthogonal in a 22-plex subset panel (Fig. 5d).

Next, we applied one round of multiplexed stoichiometric tuning on a 24-plex panel (Fig. 5e and Supplementary Note 10), with goal of achieving uniform 50% yield. After tuning, yields varied between 25% and 70% (except 1 outlier at 127%). The multiplex and pre-equilibrium nature of the assay likely reduced quantitative predictability of tuning; however, the qualitative improvement indicates that further rounds of tuning could result in improved uniformity.

Finally, we designed a 14-plex panel against cancer driver mutation sequences[23]. Paired in vitro transcript targets (250 nt containing local sequence) were used to characterize SNV selectivity (Fig. 5f). One round of stoichiometric tuning was applied to improve specificity (Supplementary Note 11). In all but 1 case (*NFE2L2-R34Q*), toehold probes and stoichiometric tuning significantly increased the selectivity (Fig. 5g).

Kinetics and use as PCR primers

To clarify confusion in the literature[24], the toehold probe displacement reaction has speed comparable to direct hybridization, given a sufficiently long (e.g. 7 nt) single-stranded toehold[25]. To demonstrate kinetics, we constructed toehold PCR primers and amplified from 2 ng human genomic DNA (Supplementary Note 13). The observed quantitation cycles (*Cq*) for toehold primers were not significantly different from single-stranded primers, indicating that strand displacement proceeds to near completion within 30 seconds at 200 nM primer concentrations.

Discussion

We have introduced and experimentally validated stoichiometric tuning as an effective, predictable, and flexible method to modulate yield and selectivity of hybridization. Compared to traditional sequence-based probe adjustment, stoichiometric tuning does not require synthesis of new molecules, allowing on-the-fly modulation of the affinity and selectivity tradeoff. Compared to empirical adjustment of assay conditions such as temperature and buffer conditions, stoichiometric tuning allows decoupled adjustment of

individual probes within multiplexed settings. As far as we are aware, this is a fundamentally novel and useful capability for multiplexed analysis of nucleic acids.

Our analyses of stoichiometric tuning assume reaction equilibrium, and may be less quantitatively predictive for applications that require pre-equilibrium readout. Kinetic simulation of underlying hybridization reactions may inform probe formulation or design for pre-equilibrium assays[8], but may be impractical for highly multiplexed systems. Our Nanostring results show that even in pre-equilibrium assays without perfect quantitative predictability, stoichiometric tuning can be useful in equalizing yields and improving SNV selectivity.

Oligonucleotide synthesis is imperfect, and even with HPLC purification, up to 15% of the molecules may harbor nucleotide deletions and/or truncations. We believe that these impurities are the main cause of the deviation between the experimental and theoretically predicted Yield vs. $[P]_0/[PC]_0$ curve (Fig. 1d and Supplementary Note 12). Nonetheless, our analyses and experiments indicate that, regardless of impurity fractions, there exists a $[P]_0/[PC]_0$ ratio that produces any desired ΔG_{eff}.

We envision that hybridization probes and primers used for a variety of nucleic acid analytic and diagnostic applications may benefit from stoichiometric tuning. For example, allele-specific PCR primers may benefit from a controllable tradeoff between mutation sensitivity and amplification efficiency (i.e. *Cq* delay), and hybrid-capture probes for NGS target enrichment[27] could benefit from yield uniformity or allele-specific enrichment. Direct hybridization assays, such as those based on fluorescent barcodes[22,26], label-free detection[28,29], or *in situ* hybridization, may be most easily adapted for stoichiometric tuning.

Supplementary Material

Refer to Web version on PubMed Central for supplementary material.

Acknowledgments

The authors thank J. H. Bae for providing assistance with qPCR instrument correction. This work was partially funded by the Rice University Department of Bioengineering startup fund to DYZ and NIH Grant EB015331 to DYZ. This work was partially funded by the Nanostring Technologies R&D team.

References

1. Mamanova L, Coffey AJ, Scott CE, Kozarewa I, Turner EH, Kumar A, Howard E, Shendure J, Turner DJ. Target-enrichment strategies for next-generation sequencing. Nat Meth. 2010; 7:111–118.
2. Newton CR, et al. Analysis of any point mutation in DNA. The amplification refractory mutation system (ARMS). Nucleic acids research. 1989; 17:2503–2516. [PubMed: 2785681]
3. Beadling C, et al. Combining highly multiplexed PCR with semiconductor-based sequencing for rapid cancer genotyping. The Journal of Molecular Diagnostics. 2013; 15:171–176. [PubMed: 23274167]
4. Mardis ER. A decade's perspective on DNA sequencing technology. Nature. 2011; 470:198–203. [PubMed: 21307932]
5. Shendure J, Aiden EL. The expanding scope of DNA sequencing. Nat Biotechnol. 2012; 30:1084–1094. [PubMed: 23138308]

6. 1000 Genomes Project Consortium et al. An integrated map of genetic variation from 1, 092 human genomes. Nature. 2012; 491:56–65. [PubMed: 23128226]
7. Zhang DY, Chen SX, Yin P. Thermodynamic optimization of nucleic acid hybridization specificity. Nature Chemistry. 2012; 4:208–214.
8. Wang JS, Zhang DY. Simulation-Guided Probe Design for Consistently Ultraspecific Hybridization. Nature Chemistry. 2015; 7:545–553.
9. Bonnet G, Tyagi S, Libchaber A, Kramer FR. Thermodynamic basis of the enhanced specificity of structured DNA probes. Proceedings of the National Academy of Sciences. 1999; 96:6171–6176.
10. Owczarzy R, Moreira BG, You Y, Behlke MA, Walder JA. Predicting stability of DNA duplexes in solutions containing magnesium and monovalent cations. Biochemistry. 2008; 47:5336–5353. [PubMed: 18422348]
11. Untergasser A, Cutcutache I, Koressaar T, Ye J, Faircloth BC, Remm M, Rozen SG. Primer3—new capabilities and interfaces. Nucleic acids research. 2012; 40:e115. [PubMed: 22730293]
12. Teer JK, et al. Systematic comparison of three genomic enrichment methods for massively parallel DNA sequencing. Genome Res. 2010; 20:1420–1431. [PubMed: 20810667]
13. Zheng Z, et al. Anchored multiplex PCR for targeted next-generation sequencing. Nat Med. 2014; 20:1479–1484. [PubMed: 25384085]
14. Deigan KE, Li TW, Mathews DH, Weeks KM. Accurate SHAPE-directed RNA structure determination. Proceedings of the National Academy of Sciences. 2008; 106:97–102.
15. SantaLucia J, Hicks D. The Thermodynamics of DNA Structural Motifs. Ann Rev Biochem. 2004; 33:415–440.
16. SantaLucia J, Turner DH. Measuring the thermodynamics of RNA secondary structure formation. Biopolymers. 1997; 44:309–319. [PubMed: 9591481]
17. Zuker M. Mfold web server for nucleic acid folding and hybridization prediction. Nucleic Acids Res. 2003; 31:3406–15. [PubMed: 12824337]
18. Zadeh JN, Steenberg CD, Bois JS, Wolfe BR, Pierce MB, Khan AR, Dirks RM, Pierce NA. NUPACK: Analysis and design of nucleic acid systems. J Comput Chem. 2011; 32:170–173. [PubMed: 20645303]
19. Clark MJ, Chen R, Lam HY, Karczewski KJ, Chen R, Euskirchen G, Butte AJ, Snyder M. Performance comparison of exome DNA sequencing technologies. Nature Biotechnology. 2011; 29:908–914.
20. Kim S, Misra A. SNP genotyping: technologies and biomedical applications. Annu Rev Biomed Eng. 2007; 9:289–320. [PubMed: 17391067]
21. Tyagi S, Kramer FR. Molecular beacons: probes that fluoresce upon hybridization. Nature Biotechnology. 1996; 14:303–308.
22. Geiss GK, et al. Direct multiplexed measurement of gene expression with color-coded probe pairs. Nat Biotechnol. 2008; 26:317–325. [PubMed: 18278033]
23. Forbes SA, et al. COSMIC: mining complete cancer genomes in the Catalogue of Somatic Mutations in Cancer. Nucleic Acids Res. 2010; 39:D945–D950. [PubMed: 20952405]
24. Altan-Bonnet G, Kramer FR. Nucleic acid hybridization: Robust sequence discrimination. Nature chemistry. 2012; 4:155–157.
25. Zhang DY, Winfree E. Control of DNA Strand Displacement Kinetics Using Toehold Exchange. J Am Chem Soc. 2009; 131:17303–17314. [PubMed: 19894722]
26. Pregibon DC, Toner M, Doyle PS. Multifunctional encoded particles for high-throughput biomolecule analysis. Science. 2007; 315:1393–1396. [PubMed: 17347435]
27. Gnirke A, et al. Solution hybrid selection with ultra-long oligonucleotides for massively parallel targeted sequencing. Nature biotechnology. 2009; 27:182–189.
28. Das J, Ivanov I, Montermini L, Rak J, Sargent EH, Kelley SO. An electrochemical clamp assay for direct, rapid analysis of circulating nucleic acids in serum. Nature Chemistry. 2015; 7:569–575.
29. Endo T, Kerman K, Nagatani N, Takamura Y, Tamiya E. Label-free detection of peptide nucleic acid-DNA hybridization using localized surface plasmon resonance based optical biosensor. Analytical Chemistry. 2005; 77:6976–6984. [PubMed: 16255598]

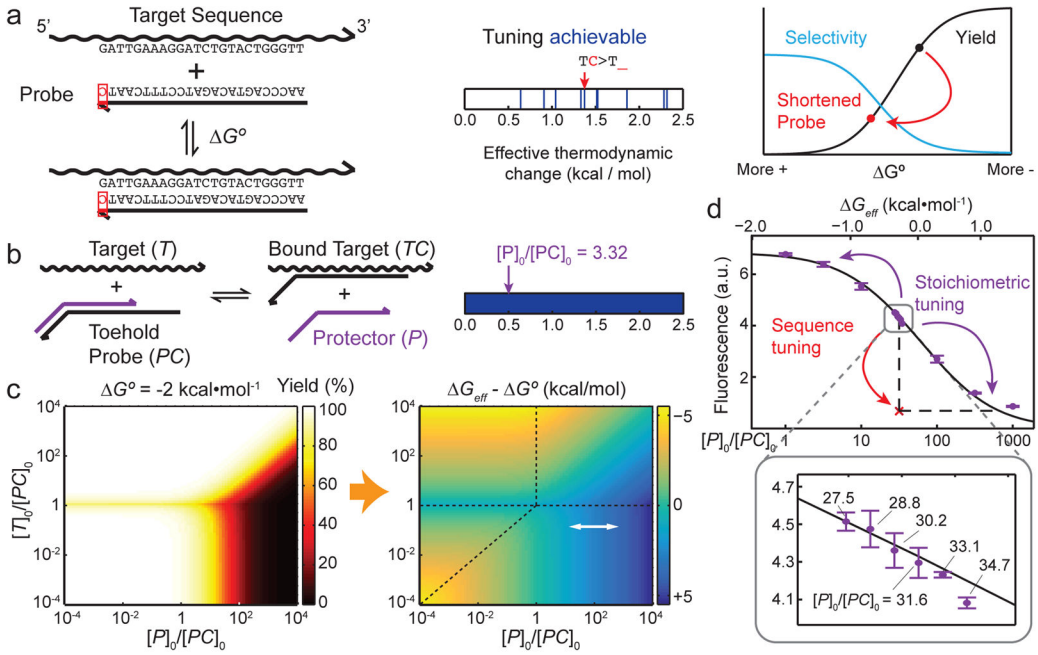

Figure 1.

Tuning the affinity-selectivity tradeoff for hybridization probes. **(a)** The standard free energy ΔG^{o}_{rxn} of a probe hybridizing to its intended target determines yield (affinity), selectivity, and melting temperature. "Sequence tuning" is the empirical adjustment of probe length; the addition or removal of each nucleotide changes ΔG^{o}_{rxn} by between 0.6 and 2.4 kcal·mol^{-1} (at 25 °C in 1× PBS), shown as blue lines in right panel[15]. **(b)** Toehold probes[7] are partially double-stranded probes that release a "Protector" strand upon hybridization to their target. The yield and selectivity of a toehold probe can be accurately and finely tuned via protector stoichiometry. **(c)** Hybridization yield χ can be stoichiometrically tuned regardless of the relative concentrations of target and probe. $[T]_0$ is the initial concentration of the target, $[PC]_0$ is the initial concentration of the probe, and $[P]_0$ is the initial excess concentration of the protector. The effective free energy $\Delta G_{eff} \equiv -R\tau \ln(\chi / (1-\chi))$ is a mapping of yield χ; the value of $(\Delta G_{eff} - \Delta G^{o}_{rxn})$ is roughly conserved regardless of the value of ΔG^{o}_{rxn}. **(d)** Experimental results on sequence and stoichiometric tuning, using a conditionally fluorescent toehold probe[7] (see Supplementary Note 3). Hybridization reactions proceeded for 12–24 hours, after which solution fluorescence was measured; kinetics experiments showed that equilibrium is achieved within 4 hours at the experimental conditions (25 °C, 1× PBS). Each data point (purple dot) shows the mean observed fluorescence at a particular stoichiometry $[P]_0/[PC]_0$ ($n = 3$); error bar shows ±1 standard deviation. The black sigmoidal curve shows the predicted (analytical) yield based on the best-fit reaction $\Delta G^{o}_{rxn} = -2.15$ kcal·mol^{-1}. The red cross shows the observed fluorescence for a toehold probe with the protector lengthened by 1 nt. $[T]_0 = 200$ pM and $[PC]_0 = 100$ pM. Inset shows zoom-in of 6 sets of experiments with $[P]_0/[PC]_0$ spaced by $10^{0.02}$ (4.7%).

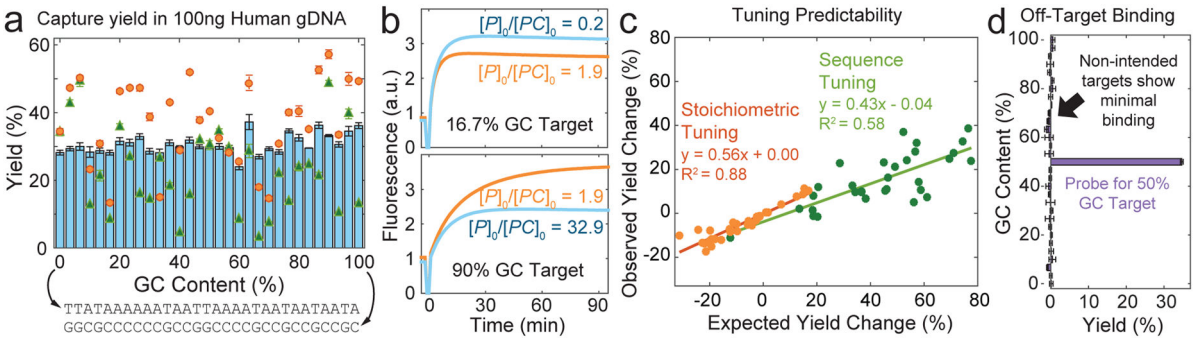

Figure 2.

Stoichiometric tuning for capture yield uniformity. **(a)** 31 distinct X-probes (Supplementary Note 5) were designed to 31 DNA targets with GC content ranging from 0% to 100%. $[T]_0$ = 150 nM and $[PC]_0$ = 200 nM. Green dots show the initial yields of these probes with stoichiometry $[P]_0/[PC]_0$ = 1.9; yields ranged from 13.3% to 61.3%. Orange dots show the yields after 1 round of sequence tuning, and bars show yields after 2 rounds of stoichiometric tuning. Optimized $[P]_0/[PC]_0$ ratios resulted in yields ranging between 26.6% and 36.8%. The presence of 100 ng genomic DNA showed no significant impact on capture yields. **(b)** Kinetic traces for capture of two targets with their corresponding probes, before (orange) and after (blue) stoichiometric tuning. **(c)** Relative effectiveness and predictability of sequence and stoichiometric tuning. Sequence tuning showed lower slope (indicating lower tuning effectiveness) and lower correlation constant R^2 (lower precision). **(d)** Probes show insignificant off-target binding; sequences that differ from Target by a even single nucleotide were not captured.

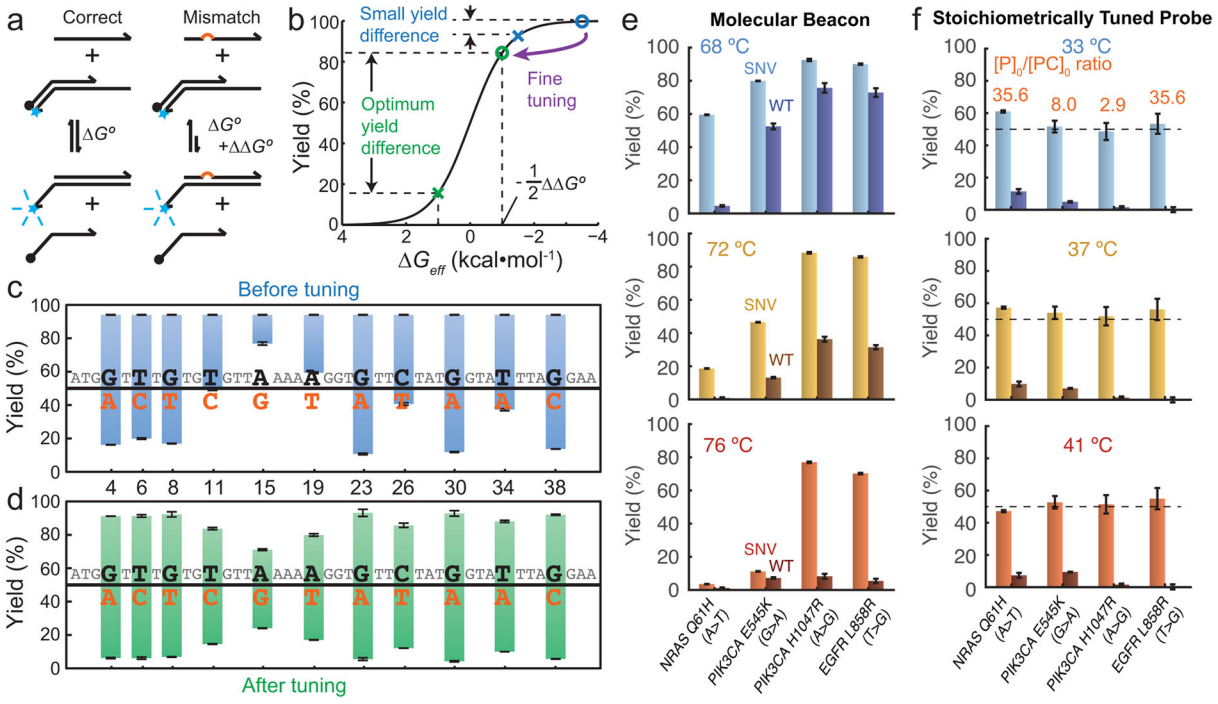

Figure 3.

Optimizing single nucleotide variant (SNV) discrimination using stoichiometric tuning. **(a)** Two SNV sequences bind to a probe with slightly different ΔG^{o}_{rxn}; the difference is referred to as the $\Delta\Delta G^{o}$. **(b)** The same $\Delta\Delta G^{o}$ value produces different changes in yield ($\Delta\chi$) based on ΔG_{eff} of the intended Target; $\Delta\chi$ is maximized when $\Delta G_{eff} \approx -\Delta\Delta G^{o}/2$ (Supplementary Note 6). **(c)** Observed yields for intended Target (top edge of bars) and 11 SNVs (bottom edges of bars), at $[P]_0/[PC]_0 = 1$. All experiments were performed in triplicate at 5× PBS at 37 °C; $[T]_0 = 200$ nM and $[PC]_0 = 100$ nM. **(d)** Yields after stoichiometric tuning. Different $[P]_0/[PC]_0$ ranging from 1.8 to 15 were used for each SNV pair. The range of $\Delta\chi$ was improved from 17.2 – 83.3% to 47.0 – 88.6%. **(e)** SNV selectivity of molecular beacons at 68 °C, 72 °C, and 76 °C, against wildtype (WT) sequences differing by a single nucleotide. The temperatures are each close to the melting different of one of the molecular beacons (Supplementary Note 7). It is impossible to achieve high SNV specificity for all three targets at any temperature, without changing molecular beacon sequences. **(f)** SNV selectivity of stoichiometrically tuned X-probes at 33 °C, 37 °C, and 41 °C. We observe resilient specificity and yield uniformity across a temperature window of at least 8 degrees.

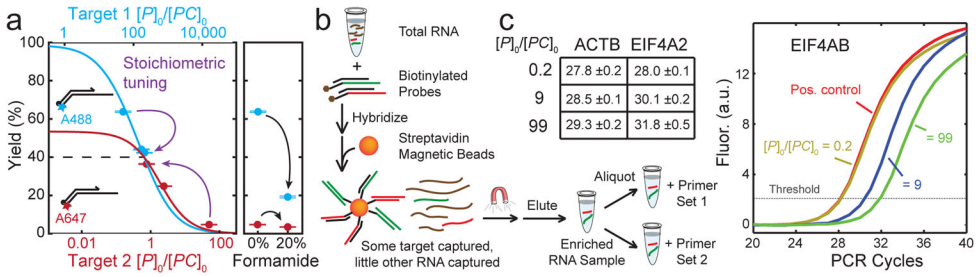

Figure 4.

Independent stoichiometric tuning in multiplex assays. **(a)** Two-plex stoichiometric tuning assayed using two toehold probes functionalized with the spectrally distinct Alexa488 and Alexa647 fluorophores. Initial $[P]_0/[PC]_0 = 50$ formulations resulted in 64% and 5% yield, respectively. Stoichiometrically tuning the probes to $[P]_0/[PC]_0 = 208$ and 0.765, respectively, adjusted binding yield to roughly 40% for both targets (n=3). In contrast, increasing formamide concentration decreases yield for both targets in a coupled manner. **(b)** Multiplex hybrid-capture of 2 mRNA species, *ACTB* (Actin beta, NM_001101.3-pos. 1673–1709) and *EIF4A2* (Eukaryotic translation initiation factor 4A2, NM-001967.3-pos. 1640–1675), from total RNA using magnetic beads. **(c)** Reverse transcription quantitative PCR (RT-qPCR) analysis of hybrid-capture efficiency; shown in the table are quantitation cycle (*Cq*) values for each of the two targets. With higher $[P]_0/[PC]_0$ ratios, less RNA is captured, consistent with theory.

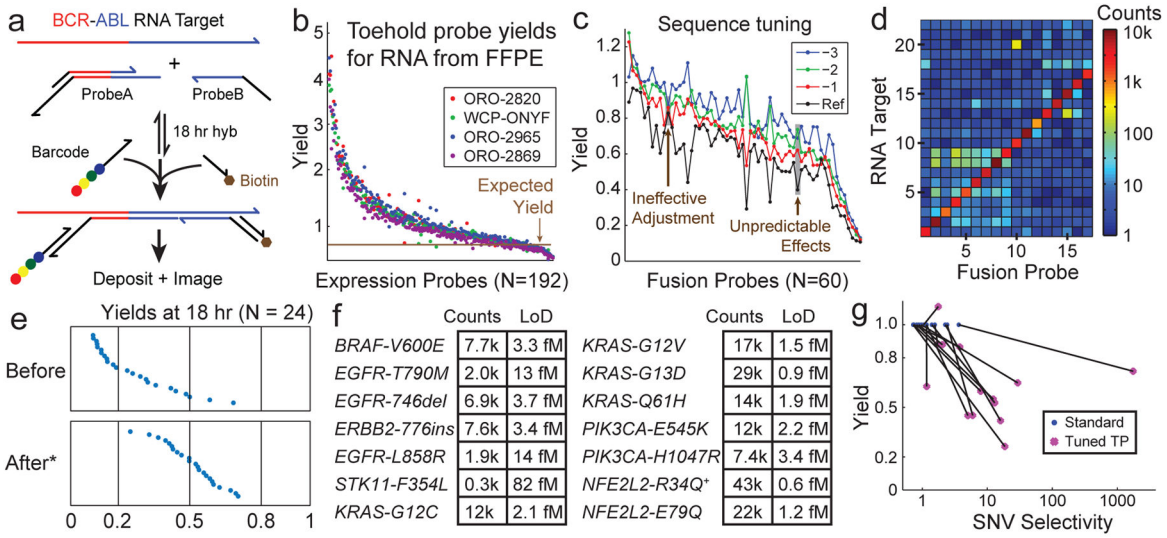

Figure 5.

Multiplexed RNA quantitation with the Nanostring nCounter. **(a)** Two hybridization probes (ProbeA and ProbeB) tether a fluorescent barcode and a biotin, respectively, to an RNA target; subsequent wash and fluorescence imaging shows single-molecule detection of the targets. ProbeA is modified into a toehold probe to confer increased specificity and to enable stoichiometric tuning. **(b)** Calibration of toehold probe system on RNA extracted from 4 distinct FFPE samples, using a 192-plex gene expression panel. Each probe individually designed to achieve 50% yield at $[P]_0/[PC]_0 = 1$. Observed yields shown here are normalized to $\chi = 1$ for unprotected probes. **(c)** Sequence tuning on 60-plex toehold probe panel for *BCR-ABL* fusion transcripts (Supplementary Note 9). Four variants of each probe were tested: the protectors successfully truncated to produce ΔG^{o}_{rxn} values 1, 2, and 3 kcal·mol^{-1} more favorable than the reference toehold probe. For a minority of probes, sequence tuning was ineffective or unpredictable. **(d)** Crosstalk analysis of subset of fusion panel. Note the logarithmic nature of the colormap scale. **(e)** 24-plex stoichiometric tuning. Initial yields showed 8-fold high-to-low variability (9% to 68%); through 1 round of tuning, yield variability was reduced to 3-fold (25% to 70%), with the exception of one outlier that gave 127% yield. **(f)** Selective detection of 14 clinically important SNVs, insertions, and deletions. Targets are in vitro transcribed RNA (256 fM each). Limit of detection (LoD) is based on 100 counts being a minimum definitive positive signal. [+]The *NFE2L2-R34Q* did not yield significant discrimination between the Target and the wildtype. **(g)** Summary of yield and SNV selectivity effects of stoichiometrically tuned toehold probes (TP). Selectivity is calculated as Counts observed for Target RNA divided by Counts for an equal concentration of wildtype RNA.